Speckle reduction process based on digital filtering and wavelet compounding in optical coherence tomography for dermatology

Juan J. Gómez-Valverde[a,b], Juan E. Ortuño[b,a], Pedro Guerra[a,b], Boris Hermann[c], Behrooz Zabihian[c], José L. Rubio-Guivernau[d], Andrés Santos[a,b], Wolfgang Drexler[c], María J. Ledesma-Carbayo[a,b]
[a]Department of Electronic Engineering, ETSI Telecomunicación, Universidad Politécnica de Madrid, Spain;[b]Biomedical Research Center in Bioengineering, Biomaterials and Nanomedicine (CIBER-BBN), Spain;[c]Center for Medical Physics and Biomedical Engineering, Medical University of Vienna, Austria;[d]MedLumics S.L Tres Cantos (Madrid), Spain

ABSTRACT

Optical Coherence Tomography (OCT) has shown a great potential as a complementary imaging tool in the diagnosis of skin diseases. Speckle noise is the most prominent artifact present in OCT images and could limit the interpretation and detection capabilities. In this work we propose a new speckle reduction process and compare it with various denoising filters with high edge-preserving potential, using several sets of dermatological OCT B-scans. To validate the performance we used a custom-designed spectral domain OCT and two different data set groups. The first group consisted in five datasets of a single B-scan captured N times (with N<20), the second were five 3D volumes of 25 B-scans. As quality metrics we used signal to noise (SNR), contrast to noise (CNR) and equivalent number of looks (ENL) ratios. Our results show that a process based on a combination of a 2D enhanced sigma digital filter and a wavelet compounding method achieves the best results in terms of the improvement of the quality metrics. In the first group of individual B-scans we achieved improvements in SNR, CNR and ENL of 16.87 dB, 2.19 and 328 respectively; for the 3D volume datasets the improvements were 15.65 dB, 3.44 and 1148. Our results suggest that the proposed enhancement process may significantly reduce speckle, increasing SNR, CNR and ENL and reducing the number of extra acquisitions of the same frame.

Keywords: Optical coherence tomography, speckle, digital filtering, denoising, dermatology

1. INTRODUCTION

Optical coherence tomography (OCT) is a non-invasive technique that presents a view of the superficial layers of tissue in vivo and in real-time [1]. It is broadly used as a diagnostic tool in ophthalmology since its introduction and has been proven as a useful tool in other specialties like dermatology for the diagnosis of skin diseases. In particular OCT has shown promising results as a non-invasive alternative to excisional biopsy helping in the detection of tumors, such as malignant melanoma and basal cell carcinoma, complementing other imaging tools such as dermatoscopy or confocal laser scan microscopy [2, 3]. Speckle noise is the most prominent artifact present in OCT images. It limits the interpretation and diagnosis and reduces the contrast and the signal to noise ratio (SNR) [4]. In images of highly scattering biological tissues, speckle has a dual role as a source of noise and a carrier of information on tissue microstructure. So special care should be taken, because removing the speckle could imply deleting useful information.

Much work has been performed for reducing speckle noise. We can make a first classification of speckle reduction techniques in software and hardware solutions. The hardware based techniques require the modification in the optical setup or change of scanning protocols. The goal is to obtain several tomograms that are averaged to get final images with a reduction in speckle contrast. The main challenge of these methods is to acquire images in a way that the speckle pattern changes, but produce a minimum alteration of the image structure. We can divide hardware techniques into serial and parallel [5]. The parallel hardware speckle reduction methods acquire tomograms with different speckle patterns used for averaging at the same time. The differentiation of speckle patterns has been achieved applying light with different polarizations emitted by two sources [6], by frequency compounding, with the incoherent summation of the magnitudes of two incoherent interferometric signals recorded at two different center wavelengths simultaneously [7], using a partially spatially coherent source [8]. The serial technique is simpler. It consists in the acquisition of several B-scans in consecutive time intervals from the same location of the sample, but with a slightly changed ensemble of the illuminated scattering particles [5, 9]. Another popular approach of differentiating speckle pattern is averaging

Optical Coherence Imaging Techniques and Imaging in Scattering Media, edited by Brett E. Bouma, Maciej Wojtkowski, Proc. of SPIE-OSA Biomedical Optics, SPIE Vol. 9541, 95411K · © 2015 SPIE-OSA · CCC code: 1605-7422/15/$18 · doi: 10.1117/12.2183815

tomographic images acquired from different observation angles. This method is usually known as "angular compounding" and has been developed in several modalities, using path length encoding and averaging images obtained at different incident angles with each image encoded by path length [10], through Doppler encoding [11] or using multiple backscattering angles encoding [12]. Finally in the last few years several methods have been proposed to improve the lateral resolution beyond the diffraction limit using structured interferences in a similar way as in confocal microscopy [13, 14].

Software based speckle reduction techniques have as main advantage that they could be applied to almost all 2D and 3D images acquired by an OCT device without changing the acquisition setup. The drawback is that they could need high computation needs and could affect the resolution of the image. We can include in this group multiple methods like local averaging over neighboring A-scans of each tomogram [15], averaging multiple B-scans [16], applying rotation kernel transformations to each tomogram [17], wavelet transform [4, 18, 19], image regularization [20], curvelet transform [21, 22], complex diffusion filtering [23], or digital filtering the B-scans [4] which is the approach followed in our study.

2. METHODS

2.1. Denoising filters

In this study we define a new process for speckle reduction based on the assessment of several denoising filters and their potential use in dermatological OCT imaging. We include in the evaluation well known 2D filters previously used in speckle reduction, such as versions of Enhanced Sigma (ES) [24], Adaptive Wiener (AW) [25], Median [25], Adaptive Wavelet Thresholding (AWT) [26] filters and the more recent Stein's unbiased risk estimate (SURE) method [27]. We also evaluate the combination of previous 2D filters with B-Scan fusion based on wavelets decomposition (WFS) [28] and wavelet denoising considering multiple B-scans (WMF) [29] to prove the improvement of this strategy with respect to just filtering 2D B-scans or just compounding multiple B-scans. Finally we propose the best combination of all the filters assessed in the resulting denoising process.

The Sigma Filter, also known as Lee Filter [30], is based on the two-sigma probability of Gaussian distribution and incorporates the speckle multiplicative noise model. Besides its simplicity it provides a good balance between filtering accuracy and computational complexity. We use an implementation that improves the preservation of small edges decomposing the image in several components and applying the sigma filter (ES) to them. Adaptive Wiener filter (AW) calculates the local mean, the variance and the noise power estimation and uses these local statistics adaptively to generate a pixelwise Wiener filter. The Adaptive Wavelet Thresholding (AWT) performs a discrete wavelet transform and estimates the noise standard deviation from the detail coefficients at the first level, defines an adaptive threshold based on the previous estimation and a penalization method provided by Birgé-Massart, applies a global soft threshold to the coefficients and finally performs the inverse discrete wavelet transform [5]. The value of the median filter in suppression of impulsive noise has long been recognized. Median filtering is often effective for speckle reduction. It uses the median intensity in a suitable sized and shaped region W_{ij} surrounding the pixel (i,j) of interest; hence it eliminates any impulsive artifacts with an area (in pixels) less than half the region size $||W_{ij}||$. The Stein's unbiased risk estimate (SURE) method is a new approach to orthonormal wavelet image denoising. The algorithm parametrizes the denoising process as a sum of elementary nonlinear processes with unknown weights. The method uses a priori estimation of the Mean Square Error (MSE) resulting from an arbitrary processing of noisy data. Instead of the usual strategy of the wavelet denoising method that involves statistical description of the coefficient distribution, an estimation of the statistical parameters and a search of the best denoising algorithm based on them, this filter takes advantage of Stein´s MSE estimate and goes directly to the last step, without considering the statistical description or making explicit hypotheses on the clean image.

Finally as we work with 3D volumes (sets of multiple B-scans), we have also evaluated two methods based on compounding strategies. The Image Fusion (WFS) based on wavelet decomposition transforms the original images (adjacent B-scans in our study) combines the coefficients on the transformed space and then applies the inverse transform to obtain the final result [28]. The Wavelet Multiframe (WMF) algorithm [29] uses wavelet decompositions of single frames for a local noise and structure estimation. Based on this analysis, the wavelet detail coefficients are weighted, averaged and reconstructed. In both cases we use two consecutive frames (or B-scans) to perform the calculations.

2.2. Quality metrics

We evaluate filter performance through common speckle-reduction performance metrics [4, 18, 20, 31] including Signal to Noise Ratio (SNR), Contrast to Noise Ratio (CNR) and Equivalent Number of Looks (ENL) which is a measure of the smoothness of homogeneous regions of interest and Edge-Enhancing Index (EEI) to assess the ability to enhance edges. Signal to Noise Ratio (SNR) or Peak Signal to Noise Ratio is defined as:

$$SNR = 10\log(\frac{\max(I^2)}{\sigma^2}) \tag{1}$$

where I is the pixel value of the target OCT image, and σ^2 is its noise variance. Contrast to Noise Ratio is:

$$CNR = \left(\frac{1}{R}\right)\sum_{r=1}^{R}(\mu_r - \mu_b)/\sqrt{\sigma_r^2 + \sigma_b^2} \tag{2}$$

where μ_b, σ_b^2 are the mean and variance in a background noise region. μ_r, $\sigma_r^2$are the mean and variance of all regions of interest (R), including the homogeneous and heterogeneous regions of interest. Equivalent Number of Looks (ENL) is a measure of the smoothness of a homogeneous region of interest:

$$ENL = (\frac{1}{H})\sum_{h=1}^{H}(\mu_h^2 / \sigma_h^2) \tag{3}$$

where μ_h, $\sigma_h^2$are the mean and variance of all homogeneous regions of interest (H). Except for the SNR calculations, all the other parameters were computed from the logarithmic OCT images.

Finally Edge-Enhancing Index is defined as:

$$EEI = \sum_{n=1}^{N}|R_{f1} - R_{f2}| \Big/ \sum_{n=1}^{N}|R_1 - R_2| \tag{4}$$

where R_1 and R_2 represent the original values of the pixels on either side of the edge, and R_{f1} and R_{f2} are the corresponding filtered values over region of interest with edges (N).

To assess the influence of all the quality metrics we consider an average Figure of Merit over all the regions of interest considered.

$$FOM = SNR_n + ENL_n + CNR_n + EEI_n \tag{5}$$

where n refers to the fact that the image quality is normalized, i.e. the filter that performed the best in, for example, the SNR criteria, SNR_n is equal to one. Therefore FOM of 4 indicates that the filter performed the best in all the image quality ratios (SNR, CNR, ENL and EEI).

3. EXPERIMENTS AND RESULTS

Five dataset with 25 B-scans (1000x680 pixels) and five dataset with N B-scans (800x1400 pixels and N<20) of the same location for the quantitative evaluation were acquired by scanning a dermatological human in-vivo tissue with a custom-designed spectral domain OCT system operating in the 1300 nm wavelength region. The broadband superluminescent diode operated at a center wavelength of 1320 nm and had a full-width at half-maximum bandwidth of 100 nm. The system was capable of providing axial and transverse resolutions of 8 µm and 20 µm respectively. Typical scanning dimensions covered a volume of 7x3.5x1.5 mm3 (1024x512x1024 voxels). The speckle reduction process proposed includes four main steps.

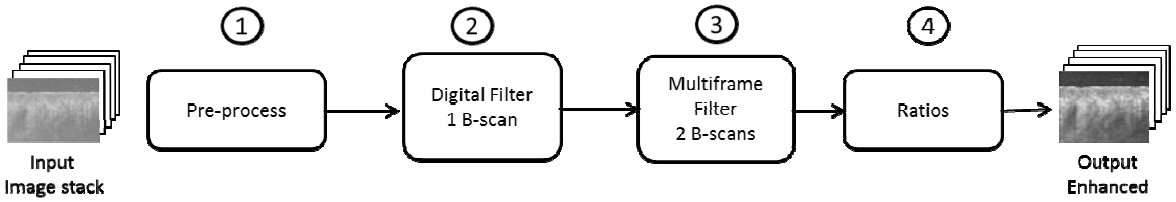

Figure 1. Speckle Reduction Process for dermatological OCT images. The input of the process is a stack of B-scans. The tests prepared in this study considered 3D volumes and single B-scans acquired multiple times.

The pre-processing step consists in the alignment of the image stack, adjusting each A-line of each image to keep the edge between the skin and the air constant in all the images.

The next step is the digital filtering of each B-scan before the B-scan compounding operation. For each individual B-scan the four digital filters described were applied: the ES filter with a window size of 5 pixels, the AW filter with window size of 5 pixels and a noise estimation based in the mode, the AWT filter with the wavelet family Coiflet 2, a level of decomposition of 3, and an estimation of the noise based on the detail coefficients of the first level. The Median filter considered the median value in a 3-by-3 neighborhood around the corresponding pixel. Finally for the SURE method we used the wavelet family Coiflet 2. The detail description of the previous parameters is beyond the scope of this paper. A complete description of these methods can be found in [24-29].

In the third step we apply the two proposed compounding filters (WFS and WMF) with groups of two adjacent B-scans previously filtered. For WFS we use the wavelet family Coiflet 1, the maximum fusion method for the approximation coefficients, the minimum for the details component and a level of decomposition equal to 6. For WMF we use 5 as decomposition levels, the Haar basis family, p controlling the noise reduction of 1.1 and as weight mode a combination of significance and correlation weights.

Finally we calculate the quality metrics (SNR, CNR, ENL and EEI) and display the results. The original raw B-scans quality metrics are shown in Table 1. Tables 2 show the subsequent improvement of the quality metrics with respect to these values except EEI which always compares the filtered and the original values (see (4)).

SNR(dB)		***CNR***		***ENL***		***EEI***
Set 1	***Set 2***	***Set 1***	***Set 2***	***Set 1***	***Set 2***	***Set 1***
21.96±0.76	23.47±0.17	1.21±0.17	1.45±0.12	60±7	42±11	20.92±2.43

Table 1. Mean ± Standard Deviation of the initial values of the quality metrics of the five 3D datasets (Set 1) and the five 2D datasets (Set 2) used for the evaluation of the speckle reduction process.

The results show that all the denoising filters improve the image quality metrics (SNR, CNR, ENL and EEI). The best results are accomplished using the combination of digital filtering individual B-scans with the Enhanced Sigma Filter followed by the image compounding of two consecutive B-scans using the WMF algorithm (Table 2).

Filter Name	***SNR(dB)***		***CNR***		***ENL***		***EEI***
	Set 1	***Set 2***	***Set 1***	***Set 2***	***Set 1***	***Set 2***	***Set 1***
ES/WMF	15.65±3.44	16.87±2.66	3.44±0.68	2.19±0.12	1148±239	328±98	2.25±0.2
AWT/WMF	15.91±4.15	13.27±1.5	3.04±0.53	2.14±0.17	980±331	255±117	1.88±0.15
AW/WMF	15.37±3.84	13.27±1.73	2.97±3.84	2.28±0.15	916±322	280±100	2.09±0.16
AWT/WFS	14.74±2.72	12.46±1.13	2.86±0.59	1.97±0.15	813±241	207±89	1.62±0.15
ES/WFS	13.1±1.77	15.27±2.38	2.9±0.67	1.93±0.23	769±94	247±62	1.72±0.16
MD/WMF	13.47±2.74	10.81±2.38	2.39±0.54	1.46±0.14	612±214	139±48	2.04±0.14
AW/WFS	12.83±2.08	11.56±1.27	2.97±0.64	1.97±0.22	633±153	218±65	1.72±0.16
SURE/WMF	10.84±1.76	8.71±1.46	1.85±0.37	0.92±0.08	377±130	72±29	1.72±0.16
MD/WFS	10.15±0.87	8.70±1.38	1.84±0.38	1.25±0.08	363±64	119±38	1.61±0.13
SURE/WFS	6.98±0.45	6.04±0.56	1.19±0.25	0.74±0..07	180±32	65±25	1.39±0.11

Table 2. Mean ± Standard Deviation of the improvement of the Enhancement metrics of the five 3D datasets used for the evaluation (Set 1) and the five 2D datasets (Set 2). The filters are ordered according to their FOM ratio values.

With this strategy the quality metrics increase for all the filters and reduce the speckle noise, improving the possible study of details in the image. In figures 1 and 2 we can appreciate an example of the effect of the application of the complete speckle reduction process in two B-scans. As we can notice in the detail white boxes of figure 2, one of the advantages of this process is that it is possible to appreciate more clearly the different layers of the skin.

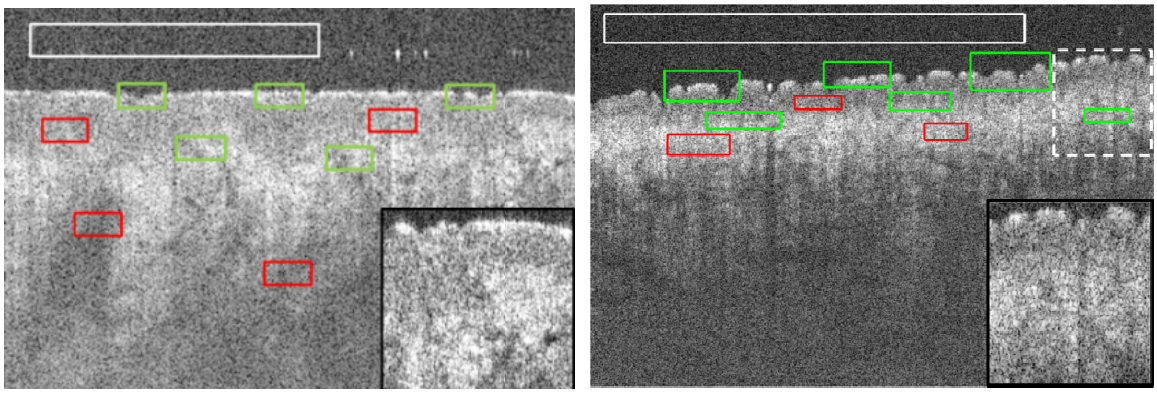

Figure 1. Dermatological OCT raw image before enhancement process (Left) B-Scan #1, Set 1, Stack 1. Initial quality metrics SNR=21.89 dB, CNR=1.16 and ENL=86.05. (Right) B-Scan #1, Set 1 Stack4. Initial quality metrics SNR=22.21 dB, CNR=1.57 and ENL=70.36. ROIs used for the calculation of the quality ratios marked. White rectangle is used for noise estimation, red rectangles represent the homogeneous regions (H=4) and green rectangles the non-homogeneous regions. The sum of both are used to calculate the CNR (R=9).

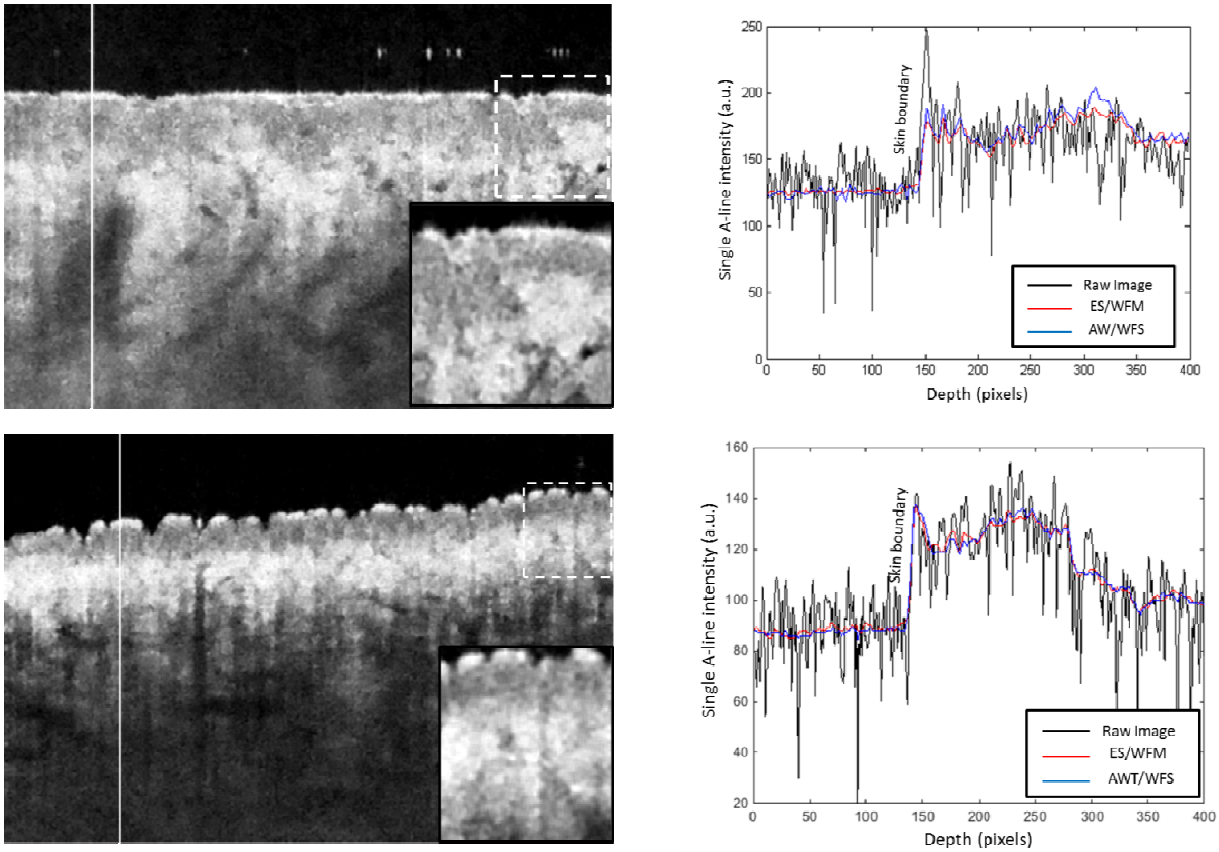

Figure 2. (First Row) Dermatological OCT image (B-Scan #1, Set1, Stack1) after applying the complete enhancement process with ES Filter followed by the WMF algorithm. Final quality metrics SNR=40.30 dB, CNR=4.57 and ENL=1563. Enhancement improvement values SNR=18.41 dB, CNR = 3.41 and ENL=1447.7. Vertical white line corresponds to A-Line #150. On the right, A-Line #150 profile of the raw image (black), the ES/WMF result (red) and AW/WFS (blue) result B-Scan #1. (Second Row) Dermatological OCT image (B-Scan #1, Set1, Stack4) after applying the complete enhancement process with ES Filter followed by the WMF algorithm. Final quality metrics SNR=40.87 dB, CNR=6.54 and ENL=919. Enhancement improvement values SNR=18.67 dB, CNR=4.96 and ENL=849. Vertical white line corresponds to A-Line #204. On the right, A-Line #204 profile of the raw image (black), the ES/WMF result (red) and AWT/WFS (blue) result B-Scan #1.

Finally the Figure of Merit of both sets considering all the metrics according with the previous results is:

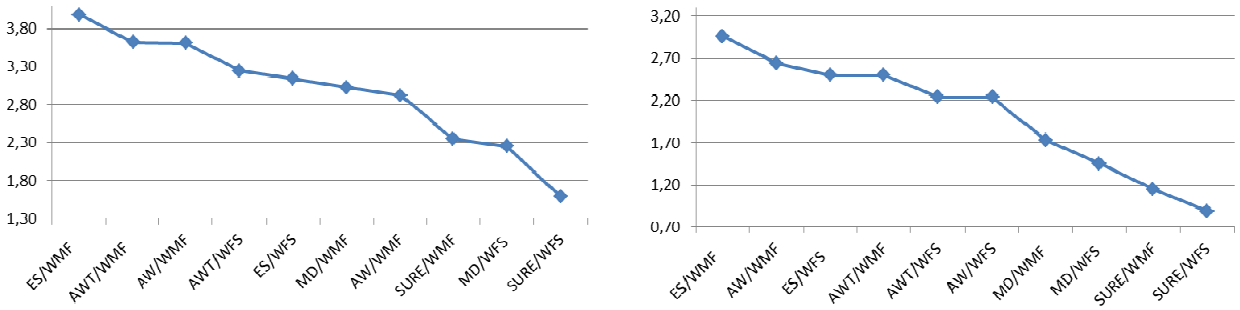

Figure 3. (Left) Figure of Merit considering the quality metrics SNR, CNR, ENL and EEI (in the Set 1) of the best digital filter methods. (Right) Figure of Merit considering the quality metrics SNR, CNR, ENL (in the Set 2) of the best digital filter methods.

CONCLUSIONS

We propose a new speckle reduction process that combines 2D digital filtering and wavelet compounding of pairs of B scans. The evaluation of this strategy with several sets of dermatological OCT images shows an improvement in all the quality metrics used in the study (SNR, CNR, ENL and EEI). The combination of the 2D ES filter and the WMF compounding filter offered the best result. Further work must be done considering the evaluation of other compounding algorithms and global computing performance issues of the global process. The qualitative assessment by specialists is also needed to confirm that the proposed enhancement scheme helps in the diagnosis of skin diseases.

ACKNOWLEDGMENTS

This work was partly supported by the European Union FP7 project BiopsyPen and by the European Fund for Regional Development (FEDER).

REFERENCES

[1] D. Huang, E. A. Swanson, C. P. Lin, J. S. Schuman, W. G. Stinson, W. Chang, M. R. Hee, T. Flotte, K. Gregory, and C. A. Puliafito, "Optical coherence tomography," *Science,* vol. 254, no. 5035, pp. 1178-1181, 1991.

[2] A. Alex, J. Weingast, B. Hofer, M. Eibl, M. Binder, H. Pehamberger, W. Drexler, and B. Povazay, "3D optical coherence tomography for clinical diagnosis of nonmelanoma skin cancers," *Imaging in Medicine,* vol. 3, no. 6, pp. 653-674, 2011.

[3] A. Alex, J. Weingast, M. Weinigel, M. Kellner-Höfer, R. Nemecek, M. Binder, H. Pehamberger, K. König, and W. Drexler, "Three-dimensional multiphoton/optical coherence tomography for diagnostic applications in dermatology," *Journal of biophotonics,* vol. 6, no. 4, pp. 352-362, 2013.

[4] A. Ozcan, A. Bilenca, A. E. Desjardins, B. E. Bouma, and G. J. Tearney, "Speckle reduction in optical coherence tomography images using digital filtering," *JOSA A,* vol. 24, no. 7, pp. 1901-1910, 2007.

[5] M. Szkulmowski, I. Gorczynska, D. Szlag, M. Sylwestrzak, A. Kowalczyk, and M. Wojtkowski, "Efficient reduction of speckle noise in Optical Coherence Tomography," *Optics express,* vol. 20, no. 2, pp. 1337-1359, 2012.

[6] H. Ren, Z. Ding, Y. Zhao, J. Miao, J. S. Nelson, and Z. Chen, "Phase-resolved functional optical coherence tomography: simultaneous imaging of< i> in situ</i> tissue structure, blood flow velocity, standard deviation, birefringence, and Stokes vectors in human skin," *Optics Letters,* vol. 27, no. 19, pp. 1702-1704, 2002.

[7] M. Pircher, E. Go, R. Leitgeb, A. F. Fercher, and C. K. Hitzenberger, "Speckle reduction in optical coherence tomography by frequency compounding," *Journal of Biomedical Optics,* vol. 8, no. 3, pp. 565-569, 2003.

[8] J. Kim, D. T. Miller, E. Kim, S. Oh, J. Oh, and T. E. Milner, "Optical coherence tomography speckle reduction by a partially spatially coherent source," *Journal of Biomedical Optics,* vol. 10, no. 6, pp. 064034-064034, 2005.

[9] T. M. Jørgensen, U. Christensen, W. Soliman, J. Thomadsen, and B. Sander, "Enhancing the signal-to-noise ratio in ophthalmic optical coherence tomography by image registration—method and clinical examples," *Journal of biomedical optics,* vol. 12, no. 4, pp. 041208-041208, 2007.
[10] N. Iftimia, G. J. Tearney, and B. E. Bouma, "Speckle reduction in optical coherence tomography by "path length encoded" angular compounding," *Journal of biomedical optics,* vol. 8, no. 2, pp. 260-263, 2003.
[11] H. Wang, and A. M. Rollins, "Speckle reduction in optical coherence tomography using angular compounding by B-scan Doppler-shift encoding," *Journal of biomedical optics,* vol. 14, no. 3, pp. 030512-030512, 2009.
[12] A. E. Desjardins, B. J. Vakoc, W. Y. Oh, S. M. Motaghiannezam, G. J. Tearney, and B. E. Bouma, "Angle-resolved optical coherence tomography with sequential angular selectivity for speckle reduction," *Optics express,* vol. 15, no. 10, pp. 6200-6209, 2007.
[13] J. Yi, Q. Wei, H. F. Zhang, and V. Backman, "Structured interference optical coherence tomography," *Optics letters,* vol. 37, no. 15, pp. 3048-3050, 2012.
[14] M. G. L. Gustafsson, "Surpassing the lateral resolution limit by a factor of two using structured illumination microscopy," *Journal of microscopy,* vol. 198, no. 2, pp. 82-87, 2000.
[15] M. Pircher, E. Götzinger, R. Leitgeb, A. Fercher, and C. Hitzenberger, "Measurement and imaging of water concentration in human cornea with differential absorption optical coherence tomography," *Optics Express,* vol. 11, no. 18, pp. 2190-2197, 2003.
[16] B. Sander, M. Larsen, L. Thrane, J. L. Hougaard, and T. M. Jørgensen, "Enhanced optical coherence tomography imaging by multiple scan averaging," *British Journal of Ophthalmology,* vol. 89, no. 2, pp. 207-212, 2005.
[17] J. Rogowska, and M. E. Brezinski, "Evaluation of the adaptive speckle suppression filter for coronary optical coherence tomography imaging," *Medical Imaging, IEEE Transactions on,* vol. 19, no. 12, pp. 1261-1266, 2000.
[18] D. C. Adler, T. H. Ko, and J. G. Fujimoto, "Speckle reduction in optical coherence tomography images by use of a spatially adaptive wavelet filter," *Optics letters,* vol. 29, no. 24, pp. 2878-2880, 2004.
[19] P. Puvanathasan, and K. Bizheva, "Speckle noise reduction algorithm for optical coherence tomography based on interval type II fuzzy set," *Optics express,* vol. 15, no. 24, pp. 15747-15758, 2007.
[20] D. L. Marks, T. S. Ralston, and S. A. Boppart, "Speckle reduction by I-divergence regularization in optical coherence tomography," *JOSA A,* vol. 22, no. 11, pp. 2366-2371, 2005.
[21] Z. Jian, L. Yu, B. Rao, B. J. Tromberg, and Z. Chen, "Three-dimensional speckle suppression in optical coherence tomography based on the curvelet transform," *Optics express,* vol. 18, no. 2, pp. 1024-1032, 2010.
[22] Z. Jian, Z. Yu, L. Yu, B. Rao, Z. Chen, and B. J. Tromberg, "Speckle attenuation in optical coherence tomography by curvelet shrinkage," *Optics letters,* vol. 34, no. 10, pp. 1516-1518, 2009.
[23] D. Cabrera Fernández, H. M. Salinas, and C. A. Puliafito, "Automated detection of retinal layer structures on optical coherence tomography images," *Optics Express,* vol. 13, no. 25, pp. 10200-10216, 2005.
[24] R. C. Bilcu, and M. Vehvilainen, "A modified sigma filter for noise reduction in images." Proc. of the 9th WSEAS International Conference on Communications. 2005.
[25] J. S. Lim, "Two-dimensional signal and image processing," *Englewood Cliffs, NJ, Prentice Hall, 1990, 710 p.,* vol. 1, 1990.
[26] S. G. Chang, B. Yu, and M. Vetterli, "Adaptive wavelet thresholding for image denoising and compression," *Image Processing, IEEE Transactions on,* vol. 9, no. 9, pp. 1532-1546, 2000.
[27] F. Luisier, T. Blu, and M. Unser, "A new SURE approach to image denoising: Interscale orthonormal wavelet thresholding," *Image Processing, IEEE Transactions on,* vol. 16, no. 3, pp. 593-606, 2007.
[28] G. Pajares, and J. Manuel de la Cruz, "A wavelet-based image fusion tutorial," *Pattern recognition,* vol. 37, no. 9, pp. 1855-1872, 2004.
[29] M. A. Mayer, A. Borsdorf, M. Wagner, J. Hornegger, C. Y. Mardin, and R. P. Tornow, "Wavelet denoising of multiframe optical coherence tomography data," *Biomedical optics express,* vol. 3, no. 3, pp. 572-589, 2012.
[30] J.-S. Lee, "Digital image smoothing and the sigma filter," *Computer Vision, Graphics, and Image Processing,* vol. 24, no. 2, pp. 255-269, 1983.
[31] F. Qiu, J. Berglund, J. R. Jensen, P. Thakkar, and D. Ren, "Speckle noise reduction in SAR imagery using a local adaptive median filter," *GIScience & Remote Sensing,* vol. 41, no. 3, pp. 244-266, 2004.